PREAMBLE-BASED SYNCHRONIZATION FOR OFDM/OQAM SYSTEMS

Davide Mattera and Mario Tanda

Dipartimento di Ingegneria Biomedica, Elettronica e delle Telecomunicazioni,
Università di Napoli Federico II,
via Claudio 21, I-80125 Napoli, Italy.
emails: { mattera , tanda } @ unina.it

ABSTRACT

The paper deals with the problem of preamble-based synchronization for OFDM/OQAM systems. Specifically, by exploiting the conjugate-symmetry property of a recently proposed preamble structure, a simple and robust procedure for timing and CFO synchronization is proposed. The root mean square error of the proposed algorithms and the overall performance of an OFDM/OQAM system exploiting them are evaluated via computer simulations.

1. INTRODUCTION

In the last years, filter-bank multicarrier (FBMC) systems have been taken into account for high data-rate transmissions over both wired and wireless frequency-selective channels. One of the most famous multicarrier modulation techniques is orthogonal frequency division multiplexing (OFDM), other known types of FBMC systems are filtered multitone systems [1] and OFDM based on offset QAM modulation (OQAM) [2, 3].

The FBMC approach complements the FFT with a set of digital filters called polyphase network (PPN) while the OFDM approach inserts the cyclic prefix (CP) after the FFT. Unlike OFDM, OFDM/OQAM systems do not require the presence of a CP in order to combat the effects of frequency selective channels. The absence of the CP implies on the one hand the maximum spectral efficiency and, on the other hand, an increased computational complexity. However, since the subchannel filters are obtained by complex modulation of a single filter, efficient polyphase implementations are possible. Another fundamental difference between OFDM and OFDM/OQAM systems is the adoption in the latter case of pulse shaping filters very well localized in time and frequency [4, 5].

OFDM/OQAM systems, as all multicarrier systems, are more sensitive to synchronization errors than single-carrier systems. In particular, the presence of carrier frequency-offset (CFO) and symbol timing (ST) estimation errors can lead to a severe performance degradation. For this reason, it is very important to derive efficient synchronization schemes. For example, in [6, 7, 8] blind CFO estimators that exploit the second-order cyclostationarity of the transmitted OFDM/OQAM signal are proposed while in [9] a synchronization scheme for data-aided ST and CFO estimation with robust acquisition properties in dispersive channels is developed.

The contribution in [10] has shown the importance of using a preamble in order to bypass the use of pilot subcarriers for channel estimation, which OFDM/OQAM cannot inherit from OFDM. Subsequently, the research about the definition of a preamble structure has led to the proposal in [11] that appears much promising since it simplifies the procedure for CFO and channel estimation, that results to be similar to that adopted for OFDM systems; moreover, it can maintain a high efficiency in short-burst transmissions. However, when the preamble defined in [11] is considered for ST estimation, the usual approach, that is, to resort to techniques able to exploit the periodic behavior of the transmitted signal within the training-symbol interval [12], may fail. In fact, the presence of the filter-bank implies that the periodic behavior of the transmitted signal longs (approximately) more than one multicarrier symbol interval.

In this paper we show that the preamble proposed in [11] presents the conjugate symmetry property (CSP) that can be exploited to derive an effective algorithm for ST estimation following a procedure similar to that previously used in [13] for OFDM systems. Therefore, by exploiting the specific structure of the preamble proposed in [11], a simple and robust procedure for ST and CFO synchronization can be obtained.

The paper is organized as follows. In Section 2 the OFDM/OQAM system model is delineated. In Section 3 the considered preamble is described. In Section 4 it is derived the ST estimator exploiting the CSP of the preamble proposed in [11]. In Section 5 the CFO estimation method and the procedure for channel estimation are described. In Section 6 the performance analysis of an OFDM/OQAM system exploiting the considered preamble-based synchronization/equalization procedure, carried out by computer simulations, is presented and discussed. Finally, conclusions are drawn in Section 7.

Notation: $j \triangleq \sqrt{-1}$, superscript $(\cdot)^*$ denotes the complex conjugation, $\Re[\cdot]$ the real part, $\Im[\cdot]$ the imaginary part, $\delta(\cdot)$ the Kronecker delta, $|\cdot|$ the absolute value and $\angle[\cdot]$ the argument of a complex number in $[-\pi,\pi)$. Moreover, lowercase boldface letters denote column vectors, $\cdot$ the scalar product, $\times$ the component-wise product between two vectors and, finally, $\mathbf{0}$ and $\mathbf{1}$ denote, respectively, the null vector and the vector whose entries are all ones.

2. SYSTEM MODEL

Let us consider an OFDM/OQAM system with M subcarriers. The received signal when the information-bearing signal $s(t)$ presents a timing offset τ, a CFO normalized to subcarrier spacing $\varepsilon = \Delta f T$ and a carrier phase offset ϕ, can be written as

$$r(t) = e^{j\frac{2\pi}{T}\varepsilon t} e^{j\phi} s(t-\tau) + n(t) \tag{1}$$

where $n(t)$ is a zero-mean complex-valued white Gaussian noise process with independent real and imaginary part, each with two-sided power spectral density N_0. The signal $s(t)$ is equal to

$$s(t) = \sqrt{\frac{M_u}{2M}} \left[s^R(t) + j s^I(t) \right] \tag{2}$$

with

$$s^R(t) = \sum_{n=0}^{N_b+N_s-1} \sum_{k\in\mathscr{A}} a_{n,k}^R e^{jk\left(\frac{2\pi}{T}t+\frac{\pi}{2}\right)} g(t-nT) \tag{3}$$

$$s^I(t) = \sum_{n=0}^{N_b+N_s-1} \sum_{k\in\mathscr{A}} a_{n,k}^I e^{jk\left(\frac{2\pi}{T}t+\frac{\pi}{2}\right)} g(t-T/2-nT) \tag{4}$$

where T is the OFDM/OQAM symbol interval, $\mathscr{A} \subset \{0,\ldots,M-1\}$ is the set of active subcarriers, the sequences $a_{n,k}^R$ and $a_{n,k}^I$ indicate the real and imaginary part of the complex data symbols transmitted on the kth subcarrier during the nth OFDM/OQAM symbol, N_b is the number of training symbols, N_s is the number of payload symbols, while $g(t)$ is the prototype filter.

The signal $s(t)$ is generated by exploiting the following efficient strategy. The discrete-time low-pass version of the transmitted signal is given by

$$s[i] \triangleq s(t)|_{t=iT_s} = \sqrt{\frac{M_u}{2M}} \left\{ s^R[i] + j s^I[i-M/2] \right\} \qquad (5)$$

where $T_s \triangleq T/M$ is the sampling interval and M_u is the size of $\mathscr{A}$. The length of the burst signal $s[i]$ is $(N_b+N_s+K-1)M+M/2$ where K is the overlap parameter, that is, the ratio between the length of the prototype filter $g(t)$ and the multicarrier symbol interval T. The term $s^R[nM+k]$ in (5) is the $(k+1)$th component of the vector $\mathbf{d}_n^{(R)}$ ($k \in \{0,\ldots,M-1\}$); such a vector-sequence is the output of the PPN:

$$\mathbf{d}_n^{(R)} = \mathbf{g}_0 \times \mathbf{b}_n^{(R)} + \mathbf{g}_1 \times \mathbf{b}_{n-1}^{(R)} + \ldots + \mathbf{g}_{K-1} \times \mathbf{b}_{n-(K-1)}^{(R)}. \qquad (6)$$

The $(k+1)$th component of the vector $\mathbf{g}_\ell$ in (6), denoted as $g_{\ell,k}$, is defined as follows

$$g_{\ell,k} = g[\ell M + k] \quad k \in \{0,\ldots,M-1\}, \;\; \ell \in \{0,\ldots,K-1\}, \qquad (7)$$

where $g[i] = g(iT_s)$, which is null for $i \notin \{0,\ldots,KM-1\}$.

Analogously, the term $s^{(I)}[nM+k]$ in (5) is the $(k+1)$th component of the vector $\mathbf{d}_n^{(I)}$ defined as the output of the PPN:

$$\mathbf{d}_n^{(I)} = \mathbf{g}_0 \times \mathbf{b}_n^{(I)} + \mathbf{g}_1 \times \mathbf{b}_{n-1}^{(I)} + \ldots + \mathbf{g}_{K-1} \times \mathbf{b}_{n-(K-1)}^{(I)}. \qquad (8)$$

The inputs $\mathbf{b}_n^{(R)}$ and $\mathbf{b}_n^{(I)}$ of the PPNs in (6) and (8) are obtained from the input vectors $\mathbf{a}_n^{(R)}$ and $\mathbf{a}_n^{(I)}$ by IFFT transformation:

$$\mathbf{b}_n^{(R)} \triangleq \text{IFFT}[\mathbf{a}_n^{(R)} \times \mathbf{w}] \qquad \mathbf{b}_n^{(I)} \triangleq \text{IFFT}[\mathbf{a}_n^{(I)} \times \mathbf{w}] \qquad (9)$$

where, for $k \in \mathscr{A}$, the kth component w_k of the M-vector $\mathbf{w}$ is $w_k = j^k$, the kth component of the vector $\mathbf{a}_n^{(R)}$ is the symbol $a_{n,k}^R$ in (3), and the kth component of the vector $\mathbf{a}_n^{(I)}$ is the symbol $a_{n,k}^I$ in (4) while, for $k \notin \mathscr{A}$, $w_k = 0$ and the components of $\mathbf{a}_n^{(R)}$ and $\mathbf{a}_n^{(I)}$ are irrelevant. A block diagram of the structure for the efficient generation of the term $s^R[i]$ in (5) is reported in Fig. 1.

3. THE CONSIDERED PREAMBLE

In this section we describe in detail the preamble structure proposed in [11] and considered in this paper.

In standard OFDM systems, the preamble is a sequence of special symbols processed by the IFFT in the transmitter and by the FFT in the receiver. In FBMC systems, we could try to repeat this procedure since IFFT and FFT are still present in the overall chain.

The sequence of real-valued M-vectors $\mathbf{a}_n^{(R)}$ in (9) is given by

$$\underbrace{\mathbf{a}^{(T)},\ldots,\mathbf{a}^{(T)}}_{N_b}, \mathbf{a}_{N_b}^{(R)}, \mathbf{a}_{N_b+1}^{(R)}, \ldots, \mathbf{a}_{N_b+N_s-1}^{(R)} \qquad (10)$$

i.e., the first N_b vectors of the sequence are equal to a known training symbol $\mathbf{a}^{(T)}$. The components of training vector $\mathbf{a}^{(T)}$ and of the payload vectors ($\mathbf{a}_n^{(R)} + j\mathbf{a}_n^{(I)}$ for $N_b \le n \le N_b+N_s-1$) have the same energy but their real parts may belong to different constellations. Formally, (10) can be written as $\mathbf{a}_n^{(R)} \triangleq \mathbf{a}^{(T)}$ for $n \in \{0,1,\ldots,N_b-1\}$ and $\mathbf{a}_n^{(R)} \triangleq \mathbf{0}$ for $n \notin \{0,1,\ldots,N_b+N_s-1\}$.

The sequence of real-valued M-vectors $\mathbf{a}_n^{(I)}$ in (9) is given by

$$\underbrace{\mathbf{0},\ldots,\mathbf{0}}_{N_b}, \mathbf{a}_{N_b}^{(I)}, \mathbf{a}_{N_b+1}^{(I)}, \ldots, \mathbf{a}_{N_b+N_s-1}^{(I)} \qquad (11)$$

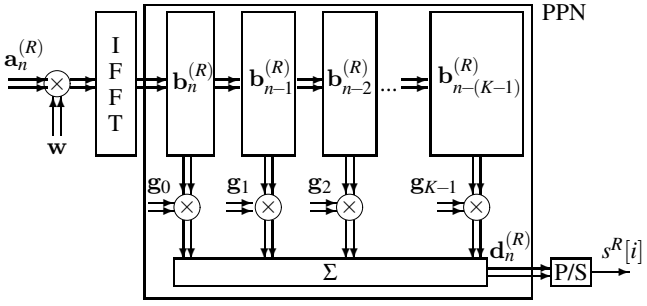

Figure 1: Structure for generating the term $s^R[i]$ in (5).

i.e., the sequence of input vectors to the PPN in (8) is null during the training period. Formally, (11) can be written as $\mathbf{a}_n^{(I)} \triangleq \mathbf{0}$ for $n \notin \{N_b,\ldots,N_b+N_s-1\}$.

In order to maintain limited the number N_b of transmitted training symbols, the preloading technique [11] is often adopted: it consists in initializing the memory of the PPN in (6) (i.e., $\mathbf{b}_n^{(R)}$ for $n \in \{-(K-1),\ldots,-1\}$) with the vector IFFT$[\mathbf{a}^{(T)} \times w]$, instead of setting it null as (10) would imply. In this case the first N_b multicarrier symbol intervals of the obtained signal $s[i]$ are equal, that is $s[i+pM] = s[i]$ for $i = 0,1,\ldots,M-1$ and $p = 0,1,\ldots,N_b-1$. With such an adoption, the transmitted preamble possesses properties that, otherwise, could be achieved only with the transmission of N_b+K training symbols. Note that the achieved efficiency can be significant: in fact, for typical values: $K=4$, $N_b=2$, and $N_s=50$, the fraction of time dedicated to preamble transmission passes from $\frac{N_b+K-1}{N_b+K-1+N_s} \simeq 9\%$ to $\frac{N_b}{N_b+N_s} \simeq 3.85\%$ while the loss of spectral containment is negligible.

4. SYMBOL TIMING ESTIMATOR

In this section we show that the previously described preamble proposed in [11] presents the CSP that can be exploited to derive an effective algorithm for ST estimation following a procedure similar to that previously used in [13] for OFDM systems.

4.1 Remind about the procedure in [13]

In OFDM systems the vector $\mathbf{w}$ in (9) has unit components, the PPN and the offset of $M/2$ samples are not present, i.e., the vector $\mathbf{d}_n^{(R)} + j\mathbf{d}_n^{(I)}$ is defined as IFFT$[\mathbf{a}_n^{(R)} + j\mathbf{a}_n^{(I)}]$ and it is transmitted after cyclic-prefix extension. Therefore, if $\mathbf{a}_n^{(I)} = \mathbf{0}$, the vector $\mathbf{d}_n^{(R)} + j\mathbf{d}_n^{(I)} = \mathbf{d}_n^{(R)}$ possesses the well-known CSP, as synthetically depicted in Fig. 2.

In the transmitted multicarrier symbol, the cyclic prefix is followed by M samples that possess the CSP: if such M samples are collected in the vector $[u_0\ \mathbf{u}_1\ u_{M/2}\ \mathbf{u}_2]$ (where both vectors $\mathbf{u}_1$ and $\mathbf{u}_2$ have $M/2-1$ components), then $\mathbf{u}_1 = \mathbf{u}_2^\#$ where $\mathbf{u}_2^\#$ denotes the flipped and conjugate version of $\mathbf{u}_2$ (i.e., the kth entry of $\mathbf{u}_1$, denoted as $u_{1,k}$, is equal to $u_{2,M/2-2-k}^*$ for $k = 0,\ldots,M/2-2$).

In the signal received on a flat channel in the absence of noise and of frequency offset, each cyclic prefix is followed by M samples that possess the CSP: if such M samples are collected in the vector $[u_0 e^{j\phi}\ \mathbf{u}_1 e^{j\phi}\ u_{M/2} e^{j\phi}\ \mathbf{u}_2 e^{j\phi}] \triangleq [v_0\ \mathbf{v}_1\ v_{M/2}\ \mathbf{v}_2]$ (where ϕ denotes the phase offset), then $\mathbf{v}_1 e^{-j\phi} = [\mathbf{v}_2 e^{-j\phi}]^\# = e^{j\phi}\mathbf{v}_2^\#$ or equivalently $\mathbf{v}_1 = e^{j2\phi}\mathbf{v}_2^\#$. Therefore, the end of the cyclic prefix and the phase offset can be determined by scanning the received signal and searching where such CSP is best approximated according to a least-squares (LS) approach, that is,

$$\left\{ \hat{\theta}^{LS}, \hat{\phi}^{LS} \right\} = \arg\min_{\theta,\phi} \|\mathbf{v}_1(\theta) - e^{j2\phi}\mathbf{v}_2^\#(\theta)\|^2 \qquad (12)$$

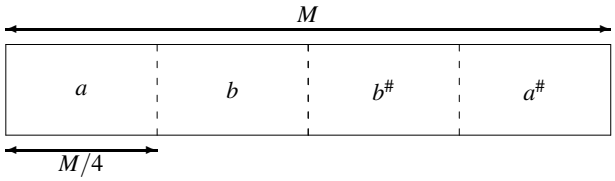

Figure 2: Structure of the OFDM symbol for $\mathbf{a}_n^{(I)} = \mathbf{0}$ [13].

where $\hat{\theta}^{LS}$ denotes the LS estimate of the normalized delay $\theta = \tau/T_s$ assumed to be an integer and, moreover, the M vector $[v_0(\theta)\ \ \mathbf{v}_1(\theta)\ \ v_{M/2}(\theta)\ \ \mathbf{v}_2(\theta)]$ has been extracted in correspondence of the candidate delay θT_s. Note that the maximization procedure in (12) provides a closed-form solution for the phase estimate $\hat{\phi}^{LS}$ and, then, the ST estimation requires only a one-dimensional search:

$$\hat{\theta}^{LS} = \arg\max_{\theta} \left\{ 2|\mathbf{v}_1(\theta)\cdot\mathbf{v}_2^{\#}(\theta)| - \|\mathbf{v}_1(\theta)\|^2 - \|\mathbf{v}_2(\theta)\|^2 \right\}. \quad (13)$$

In the following we consider a slightly different approach (modified LS (MLS)) that is aimed at simplifying the threshold setting as suggested in [14]:

$$\hat{\theta}^{MLS} = \arg\max_{\theta} \Psi(\theta) \stackrel{\triangle}{=} \arg\max_{\theta} \frac{2|\mathbf{v}_1(\theta)\cdot\mathbf{v}_2^{\#}(\theta)|}{\|\mathbf{v}_1(\theta)\|^2 + \|\mathbf{v}_2(\theta)\|^2}. \quad (14)$$

Let us note that the estimation method in (14) is robust to the the possible presence of the CFO in the received signal since both the magnitude of the scalar product and the norms in $\Psi(\theta)$ are independent of it.

4.2 Adapting the CS property to OFDM/OQAM

When the preloading technique is adopted with the considered preamble, the following property holds:

$$\mathbf{d}_0^{(R)} = \ldots = \mathbf{d}_{N_b-1}^{(R)} = [\mathbf{g}_0 + \ldots + \mathbf{g}_{K-1}] \times \mathrm{IFFT}[\mathbf{a}^{(T)} \times \mathbf{w}] \quad (15)$$

since $\mathbf{b}_n^{(R)} = \mathrm{IFFT}[\mathbf{a}^{(T)} \times \mathbf{w}]$ for $n \in \{-K+1, \ldots, -1, 0, 1, \ldots, N_b - 1\}$. If the adopted prototype filter satisfies the condition

$$\mathbf{g}_0 + \ldots + \mathbf{g}_{K-1} = \alpha \mathbf{1} \quad (16)$$

where α is a constant real value, (15) becomes

$$\mathbf{d}_0^{(R)} = \ldots = \mathbf{d}_{N_b-1}^{(R)} = \alpha \mathrm{IFFT}[\mathbf{a}^{(T)} \times \mathbf{w}]. \quad (17)$$

In the following, it will be considered the prototype filter derived in [5] by using the frequency sampling technique. It can be easily verified that the adopted prototype filter satisfies condition (16).

In OFDM/OQAM systems, as stated in Section 2, the kth component of the vector $\mathbf{w}$ in (9) is not unit but it is equal to $j^k = \exp(j2\pi\frac{1}{4}k) = \exp(j\frac{2\pi}{M}\frac{M}{4}k)$, while the vector $\mathbf{a}^{(T)}$ is real-valued; consequently, from (17) it follows that the vectors $\mathbf{d}_n^{(R)}$ $(n = 0, \ldots, N_b - 1)$ and, then, the first N_b multicarrier symbols of the preamble at the beginning of the burst, possess a conjugate symmetry that is cyclically shifted of $M/4$ samples to the left, as synthetically depicted in Fig. 3. Moreover, also in the following $K-1$ multicarrier symbol intervals such a property is partially present due to the memory of the PPN but it is partially suppressed by the effect of the contribution to $s[i]$ in (5) due to the payload symbols in the PPNs in (6) and in (8). For a typical choice of $N_b = 2$ and $K = 4$, such a property is strictly present only in the first two multicarrier symbol intervals but it is approximately present in the first three and half multicarrier symbol intervals. In fact, during the whole third interval, the loss of CSP is minimal since the contribution from $\mathbf{g}_0$ in (6) is marginal. In the fourth interval the loss becomes significant

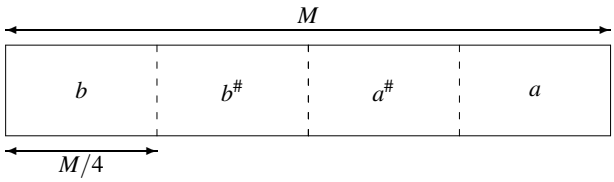

Figure 3: The structure of each of the N_b equal symbols in the considered preamble for OFDM/OQAM systems when the multiplication for $\mathbf{w}$ is taken into account (left cyclic shift).

only in the second half of the interval because the vector $\mathbf{g}_1$ dominates the sum in (6) only in the last $M/2$ components while $\mathbf{g}_2$, still multiplied by $\mathrm{IFFT}[\mathbf{a}^{(T)} \times \mathbf{w}]$, dominates the first $M/2$ components. Note that the coefficients in the last components of $\mathbf{g}_1$ and in the first components of $\mathbf{g}_2$ are those closest to the center of the prototype filter $g[i]$, which is located at the middle point $i = 2M$ of its length $4M$. When a sequence of three and half multicarrier symbols possesses the cyclically-shifted CSP, then we can detect in five positions the presence of the CSP in the overall sequence. In particular, the first of such five positions is located $M/4$ samples after the beginning of the first symbol period and the other four ones are regularly spaced and separated by $M/2$ samples. Moreover, $M/2$ samples before the first position and $M/2$ samples after the fifth position a weak CSP is detected since the property is suppressed only on half of the observed interval (for the first weak position by the noise samples proceeding the burst and for the second weak one by the second half of the fourth interval). In Fig. 4 we depict the sequence of the first three symbol periods in the transmitted signal with a symbolism that represents which parts of the discrete-time signal are the conjugate-symmetric versions of other parts. We also denote with long arrows the five positions where a strong CSP is detected in the following M samples and the two positions where a weak CSP is detected. We can therefore utilize the procedure in (14) to detect the presence of points that satisfy the CSP property and use the quantity $\Psi(\theta)$ in (14) to identify their positions; specifically, we first filter $\Psi(\theta)$ with the matched filter with impulse response:

$$\begin{aligned} h_{MF}(\theta) \stackrel{\triangle}{=} & \tfrac{1}{2}\delta(\theta - \tfrac{M}{2}) + \delta(\theta) + \delta(\theta + \tfrac{M}{2}) + \delta(\theta + 2\tfrac{M}{2}) \\ & + \delta(\theta + 3\tfrac{M}{2}) + \delta(\theta + 4\tfrac{M}{2}) + \tfrac{1}{2}\delta(\theta + 5\tfrac{M}{2}). \end{aligned} \quad (18)$$

Then, we estimate the timing offset as the position where the filter output is maximum; such a position, further reduced by $M/4+1$, provides the beginning of the burst.

In Fig. 5 we report a typical realization of the statistics $\Psi(\theta)$ in (14) in AWGN for $E_b/N_o = -3$ dB and $M = 1024$ that confirms the expected results. Although derived for the sake of clearness with reference to the special choice $K = 4$, often employed in OFDM/OQAM literature, the method can be straightforwardly extended to other values of K (and, obviously, of N_b).

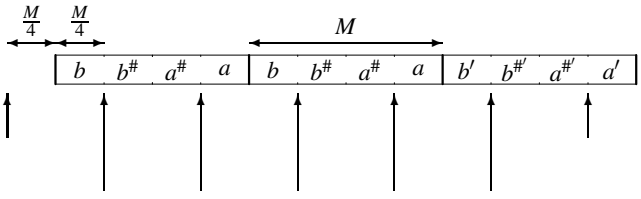

Figure 4: The structure of the first three symbol periods in the burst (two of preamble and one of payload) and the five points where a strong CSP is detected on the next M samples as well as the two points where a weak CSP is also detected. In the third symbol, the notation b' (and, obviously, $b^{\#'}$,a',$a^{\#'}$) denotes that it is not identical to b (and, obviously, to $b^{\#}$,a,$a^{\#}$, respectively) since a still negligible effect of the payload is present on such a symbol.

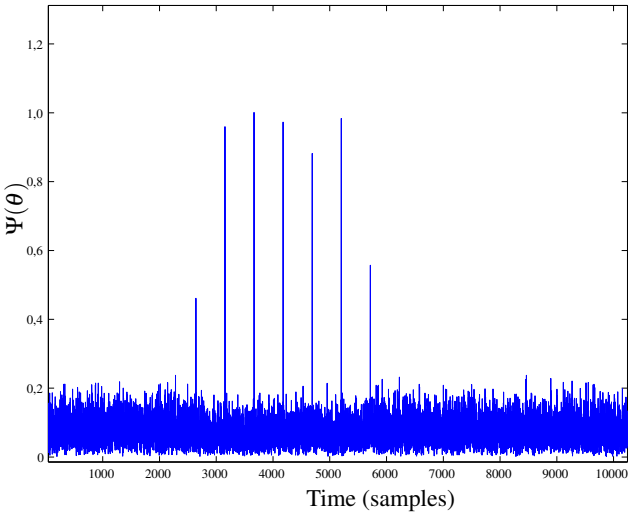

Figure 5: A typical realization of the statistics $\Psi(\theta)$ in (14) in AWGN for $E_b/N_o = -3$ dB and $M = 1024$.

5. CFO ESTIMATION AND ONE-TAP EQUALIZATION

The fact that the preamble proposed in [11] and described in Section 3 contains N_b equal multicarrier symbols can be used for synchronization and channel estimation as shown in the following.

Specifically, if $N_b \geq 2$ a CFO estimate can be obtained by using the fact that the received signal in the nth ($0 \leq n \leq N_b - 2$) multicarrier symbol period, collected in the vector $\mathbf{r}_1$, and in the $(n+1)$th one, collected in the vector $\mathbf{r}_2$, satisfy the following property in the absence of noise and of timing synchronization errors: $\mathbf{r}_2 = \mathbf{r}_1 e^{j2\pi\varepsilon}$. Therefore, the following CFO estimator can be used

$$\hat{\varepsilon} = \frac{1}{2\pi} \angle \{\mathbf{r}_2 \cdot \mathbf{r}_1\}. \tag{19}$$

Moreover, after the signal propagation over a multipath channel and neglecting the residual effects of imperfect timing and CFO synchronization, the signal received in the nth symbol interval (provided that $n \geq 1$), collected in the M-vector $\mathbf{r}$, is equal to the circular convolution of the vector $\mathbf{d}_1^{(R)}$ with the discrete-time channel impulse response. Consequently, taking into account the expression (17) for $\mathbf{d}_1^{(R)}$ and neglecting the noise, the FFT $\mathbf{R}$ of the vector $\mathbf{r}$ can be written as $\alpha \mathbf{H} \times \mathbf{a}^{(T)} \times \mathbf{w}$ where $\mathbf{H}$ is the M-vector FFT of the channel impulse response. Consequently, such a frequency response can be estimated by the following relation $\hat{\mathbf{H}} = \frac{\mathbf{R}}{\alpha \mathbf{a}^{(T)} \times \mathbf{w}}$ where the division is defined component-wise. Note that such a division has not to be performed with reference to the subcarriers not used, for which the corresponding component of $\mathbf{w}$ is null. On such subcarriers the channel frequency response cannot be estimated by using the received signal since there is no power in the transmitted signal on them. Note that an imperfect timing synchronization can imply that the signal received in the $(n+1)$th multicarrier symbol interval is only approximately equal to the circular convolution. When a simple equalizer is desired, a zero-forcing one-tap equalizer can be chosen: it can be implemented for each subcarrier exploiting the estimation of the channel frequency response.

6. NUMERICAL RESULTS

In this section the performance of an OFDM/OQAM system exploiting the proposed method for ST estimation is assessed via computer simulations. A number of 5000 Monte Carlo trials has been performed under the following conditions:

1. the considered FBMC system has a bandwidth $B = 1/T_s = 11.2$ MHz, $M = 1024$ subcarriers and overlap parameter $K = 4$;
2. the preamble is generated according to the scheme described in Section 3 with $N_b = 2$;
3. the M-vector $\mathbf{a}^{(T)}$, whose entries are antipodal symbols, is randomly generated in each trial;
4. the N_s payload symbols are the real and imaginary part of 4-QAM symbols;
5. the considered multipath fading channel models are the ITU Vehicular A and the ITU Vehicular B [15];
6. the channel is fixed in each run but it is independent from one run to another;
7. the bit-error-rate (BER) is evaluated on the fifth multicarrier symbol of the burst;
8. the timing offset is uniformly distributed in $\{3M, \ldots, 4M-1\}$, i.e., at least three symbol intervals of pure noise are included at the beginning of the transmitted signal; the overall length of the observed interval is $10M$;
9. the normalized frequency offset between transmitter and receiver is uniformly distributed in the range $[-0.45, 0.45]$.

Figure 6 displays the root mean square error (RMSE) (normalized to the number of subcarriers M) of the proposed ST estimator as a function of E_b/N_0 both in multipath channels A and B. The results show that in multipath channel A the normalized RMSE is very small while in multipath channel B is contained. It is worthwhile to emphasize that in AWGN no errors were observed in the performed 5000 trials.

Figure 7 shows that in multipath channel A the CFO estimator exploiting the proposed ST estimator assures a performance slightly different from that achieved in AWGN. The performance degradation of the ST estimator in multipath channel B leads to a corresponding degradation of the CFO estimator that is sensible only for high values of E_b/N_0.

We also analyze the effects of using the proposed synchronization on the overall system performance. In particular, in order to better single out the contribution to the overall performance of the proposed method, we analyzed six different structures for the receiver. The structure denoted with 1 is an ideal structure, which provides us an useful upper-bound to the system performance. It perfectly knows the channel to be equalized and the timing and CFO to be compensated at receiver. We also denote with 2 the structure where in the time domain the timing and CFO compensations use the estimates obtained by the proposed method while in the frequency domain the residual CFO compensation and the equalizer setting are still ideal; we denote with 3 the structure that differs from 2 only because the ideal compensation of the residual CFO in the frequency domain is not performed. The ith structure use an ideal equalizer for $i = 1,2,3$ while the structure $i+3$ is the same as i except for the use of a real one-tap equalizer, employing the coefficients obtained by the channel-estimation procedure described in Section 5. Therefore, the structure 6 is the one that can be implemented in practice. Figure 8 shows the BER of the considered six different reception structures in the presence of AWGN (denoted with W in the figure) and multipath channels ITU-A and ITU-B (denoted with A and B, respectively). We can notice that no performance loss can be directly attributed to the errors in timing estimation in the three channels since the structures 1 and 2 perform equivalently with an ideal equalizer while the structures 4 and 5 perform equivalently with the realistic equalizers. Since, as previously stated, no timing errors were observed in AWGN, the performance loss between the structures 1 and 3 (and, to a lesser extent, between 4 and 6) in AWGN is due to the residual CFO in the frequency domain, which depends on the considered multicarrier symbol interval. Therefore, mismatches in the final frequency-domain compensation (here simulated by the decision on the eight multicarrier symbol in the structures 3 and 6, which do not perform the compensation) cannot be reduced by improving the timing estimator, at least where they appear able to affect the overall performance (i.e., in AWGN). Finally, the simulation results show that, also when the residual CFO is perfectly compensated, a performance loss of 3 dB has to be ascribed to the exploitation of the measured channel in the

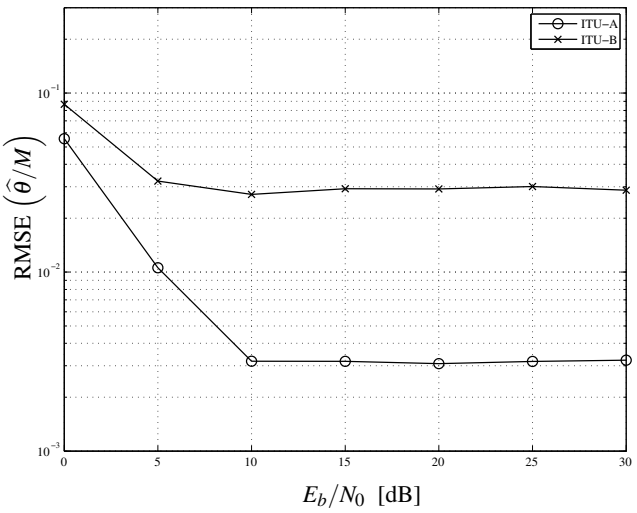

Figure 6: RMSE of the ST estimator.

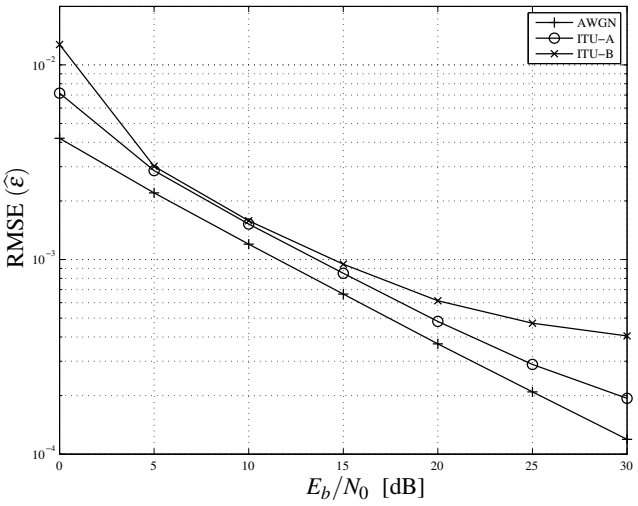

Figure 7: RMSE of the CFO estimator.

employed zero-forcing one-tap equalizer.

7. CONCLUSIONS

The problem of preamble-based synchronization for OFDM/OQAM systems has been considered. Specifically, with reference to a recently proposed structure for the burst preamble, a simple and robust procedure for timing synchronization has been proposed: it exploits the CSP of the transmitted signal, extending the method proposed in [13] for OFDM systems. The numerical results show that the proposed ST estimator, for the adopted OFDM/OQAM system and in the considered scenarios, is perfectly compatible with the use of a zero-forcing one-tap equalizer.

REFERENCES

[1] G. Cherubini, E. Eleftheriou, S. Oker, and J. Cioffi. Filter bank modulation techniques for very high speed digital subscriber lines. *IEEE Comm. Magazine*, 38(5):98–104, May 2000.

[2] B. Saltzberg. Performance of an efficient parallel data transmission system. *IEEE Trans. on Communications Technology*, 15(6):805–811, June 1967.

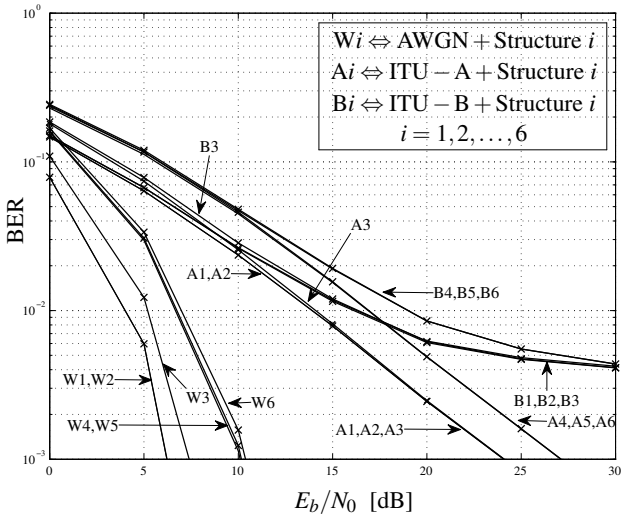

Figure 8: BER of the three considered structures on three channels (AWGN, ITU-A and ITU-B) vs $\frac{E_b}{N_0}$. The letter denotes the channel while the number specifies the receiver structure.

[3] B. L. Floch, M. Alard, and C. Berrou. Filter bank modulation techniques for very high speed digital subscriber lines. *Proc. of the IEEE*, 83(6), June 1995.

[4] P. Siohan, C. Siclet, and N. Lacaille. Analysis and design of OFDM/OQAM systems based on filterbank theory. *IEEE Trans. on Signal Processing*, 50(5):1170–1183, May 2002.

[5] M. Bellanger. Specification and design of a prototype filter for filter bank based multicarrier transmissions. *Int. Conf. on Acoustics, Speech and Signal Processing ICASSP'01*, 2001.

[6] P. Ciblat and E. Serpedin. A fine blind frequency offset estimator for OFDM/OQAM systems. *IEEE Trans. on Signal Processing*, 52(1):291–296, Jan. 2004.

[7] H. Bolcskei. Blind estimation of symbol timing and carrier frequency offset in wireless OFDM systems. *IEEE Trans. on Communications*, 49(6):988–999, Jun 2001.

[8] T. Fusco and M. Tanda. Blind frequency-offset estimation for OFDM/OQAM systems. *IEEE Trans. on Signal Processing*, 55(5):1828–1838, May 2007.

[9] T. Fusco, A. Petrella, and M. Tanda. Data-aided symbol timing and CFO synchronization for filter-bank multicarrier systems. *IEEE Trans. on Wireless Communications*, 8(5):2705–2715, May 2009.

[10] C. Lélé, J. Javaudin, R. Legouable, A. Skrzypczak, and P. Siohan. Channel estimation methods for preamble-based OFDM/OQAM modulations. *European Transactions on Telecommunications*, 2008, 2008.

[11] M. Bellanger. Efficiency of filter bank multicarrier techniques in burst radio transmission. *Proc. of IEEE Global Communications Conf. 2010 (GLOBECOMM 2010)*, Miami (FL), USA, December 2010.

[12] P. Chevillat, D. Maiwold, and G. Ungerboeck. Rapid training of a voiceband data modem receiver employing an equalizer with fractional T-spaced coefficients. *IEEE Trans. on Communications*, 35(6):869–876, September 1987.

[13] M. Tanda. Blind symbol-timing and frequency-offset estimation in OFDM systems with real data symbols. *IEEE Trans. on Communications*, 52(10):1609–1612, October 2004.

[14] H. Minn, V. Bhargava, and K. Letaief. A robust timing and frequency synchronization for OFDM systems. *IEEE Trans. on Wireless Communications*, 2(4):822–839, July 2003.

[15] Recommendation ITU-R M. 1225: Guidelines for evaluation of radio transmission technologies for IMT-2000, 1997.